ResearchGate

See discussions, stats, and author profiles for this publication at: https://www.researchgate.net/publication/248877793

Minimum Thickness Of Compacted Soil Liners: I. Stochastic Models

Article *in* Journal of Geotechnical Engineering · January 1994

DOI: 10.1061/(ASCE)0733-9410(1994)120:1(129)

CITATIONS
46

READS
119

2 authors, including:

Craig H Benson
University of Virginia

381 PUBLICATIONS **9,658** CITATIONS

SEE PROFILE

Some of the authors of this publication are also working on these related projects:

Project Containment Systems and Landfill Barriers View project

Project Dry cover material over tailing facilities View project

All content following this page was uploaded by Craig H Benson on 25 March 2018.

The user has requested enhancement of the downloaded file.

Minimum Thickness of Compacted Soil Liners: I. Stochastic Models

By Craig H. Benson[1] and David E. Daniel,[2] Members, ASCE

Abstract: Regulatory agencies often specify a minimum thickness of compacted soil liners that will ensure that the liner performs adequately. No consensus has been formed, however, on an appropriate minimum thickness. In some states soil liners may be as thin as 60 cm (2 ft), whereas in other states soil liners are required to be at least 360 cm (12 ft) thick. Difficulties encountered in the analysis of soil liners, such as uncertainties in construction, flow in macropores, and spatial variability of hydraulic properties, and variability in past experiences of regulatory agencies are the most likely reasons for the lack of consensus on minimum thickness. In the present paper, the first in a two-part series, two models of fluid flow in compacted soil liners are described. These models incorporate flow in macropores, spatial variability, and uncertainty via probability theory, but only consider advective transport in saturated soil. In the second paper, the models are used to identify an appropriate minimum thickness of soil liners.

INTRODUCTION

Compacted soil liners are earthen barriers used to minimize the movement of liquids into or from landfills, surface impoundments, and other facilities that contain materials that can contaminate groundwater. In an effort to protect the environment, regulatory agencies typically specify a minimum thickness of soil liners that will ensure the liner performs adequately. Although definitions of performance vary, adequate performance requires that a soil liner be physically stable (foundation and side slopes), have a relatively long time before leakage first occurs, and have a small flux subsequent to the commencement of leakage. No consensus has been formed, however, regarding a minimum thickness that satisfies these performance criteria. The lack of consensus is evident in wide variation in minimum thickness, 60–360 cm (2–12 ft), that has been documented by Goldman et al. (1988).

In the present paper, the first in a two-part series, the formulation, mathematical development, and verification of two models of fluid flow in compacted soil is described. The first model simulates flow as a continuum process and the second model simulates flow in macropores. Only advective transport of conservative solutes is considered. The models described in the present paper also incorporate the spatial variability of the hydraulic properties of the soil by employing probability theory; hence, they are stochastic models. Furthermore, the performance of soil liners is measured by the minimum time of travel, herein called the first-passage time, and the magnitude of the flux subsequent to first passage.

In the second paper of the series (Benson and Daniel 1994), the stochastic models are employed to evaluate the sensitivity of distributions of first-passage time and flux to the thickness of a soil liner and the hydraulic

[1]Asst. Prof., Dept. of Civ. and Envir. Engrg., Univ. of Wisconsin-Madison, Madison, WI 53706.

[2]Prof., Dept. of Civ. Engrg., Univ. of Texas at Austin, Austin, TX 78712.

Note. Discussion open until June 1, 1994. Separate discussions should be submitted for the individual papers in this symposium. To extend the closing date one month, a written request must be filed with the ASCE Manager of Journals. The manuscript for this paper was submitted for review and possible publication on November 13, 1990. This paper is part of the *Journal of Geotechnical Engineering*, Vol. 120, No. 1, January, 1994. ©ASCE, ISSN 0733-9410/94/0001-0129/$1.00 + $.15 per page. Paper No. 913.

properties of the soil. The distribution of flux (interpreted in terms of hydraulic conductivity) is compared with a statistical analysis of field measurements of hydraulic conductivity and conclusions are drawn with regard to minimum thickness.

PATTERNS OF FLUID FLOW IN SOIL

Continuum versus Discrete Flow Fields

Traditional analyses of flow in compacted soil assume that liquid flows in soil as a continuum process (Freeze and Cherry 1979). By definition, a continuum process requires that the pressure, density, and viscosity of the liquid to be functions that vary smoothly from point to point in the entire control volume (Corey 1977). The validity of a continuum analysis to describe flow in soil, however, is predicated on the assumption that the flow field is observed at a sufficiently large scale compared to the scale of the pore size and spacing. Under the assumption of a continuum, the analysis employs hydraulic conductivity and porosity as the spatially averaged properties of the soil.

Flow in Compacted Soil Liners

Patterns of flow in compacted soil are sensitive to the methods used during preparation and compaction of the soil. Some recent studies have shown that liquid flowing through compacted soil does not behave as a continuum process, but instead the liquid moves through relatively large widely spaced pores that represent only a small percentage of the total volume of the soil. These large pores, called macropores, are of irregular size and orientation and act as discrete channels for flow. Fig. 1 illustrates the patterns of flow found by several investigators (Anderson et al. 1991; Elsbury and Sraders 1989; Rogowski 1990). Through the use of dyes or tracers, the investigators have found liquid to travel vertically downward in macropores within a lift of soil, and then to spread horizontally in a planar region, called the interlift zone, that exists between adjacent lifts. The liquid continues to spread in the interlift zone until it reaches another macropore in the lower lift. It has been postulated that the ability for liquid to flow in the interlift zone has a significant effect on the performance of soil liners.

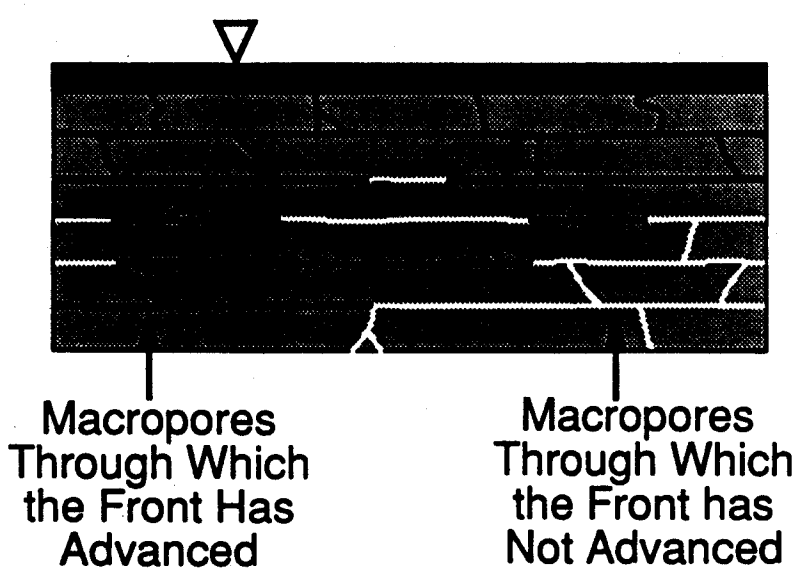

FIG. 1. Flow in Discrete Macropores in Compacted Soil Liner

The observations of these investigators are not necessarily a general representation of flow in compacted soils. The test pad constructed by Elsbury and Sraders was compacted slightly dry of optimum with a moderate size roller, which can result in incomplete remolding of clods and large interclod voids (Benson and Daniel 1990). Furthermore, the clods were large and in some instances were larger than the thickness of a lift (≈15 cm). Hence, the construction methods used by Elsbury and Sraders may have been conducive to the presence of large interclod voids. The test pads built by Rogowski (1990) and Anderson et al. (1991) were also constructed with equipment smaller than equipment ordinarily used to build soil liners. Hence, the results shown in their studies may reflect an atypical presence of undeformed clods and large interclod voids.

Other investigators have found that liquid tends to move through compacted soil as a relatively smooth, but irregular front (e.g., Albrecht et al. 1989) as shown in Fig. 2. Apparently, the soils used in these studies were compacted with heavy machinery that deformed the clods and eliminated the interclod voids during compaction. Hence, the soil was devoid of large macropores that act as conduits for rapid flow in the lifts. Undoubtedly, the voids through which the liquid flowed in these experimental liners were small and closely spaced; hence, the flow appeared to be a continuum process.

Patterns of flow in most compacted soil liners are likely to appear somewhere between the extremes of a discontinuous network of discrete macropores and a smooth continuum process. A smooth front is probably realized in well-compacted portions of the liner and flow in macropores probably occurs in regions in which the soil was processed improperly or the compactive effort was inadequate. In some regions, both types of flow fields probably exist and interact.

One-Dimensional versus Three-Dimensional Flow

Flow in any soil is three dimensional because the pores vary in orientation, but it is difficult and not always necessary to model three-dimensional flow. In a well-compacted soil liner, the flow field will exhibit some characteristics of three-dimensional flow, but the majority of the flow should be one dimensional because the hydraulic gradient is vertical and the hydraulic prop-

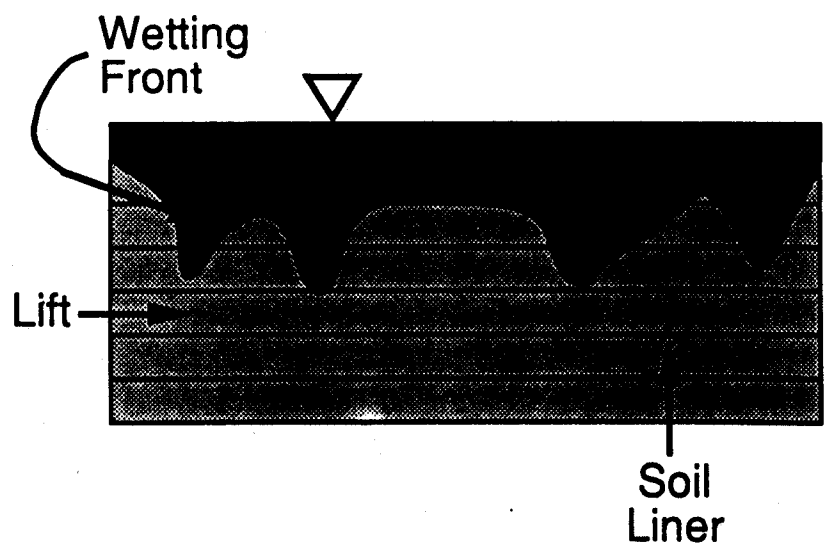

FIG. 2. Flow as Continuum Process in Compacted Soil Liners

erties vary smoothly as if the soil is a continuum. Nonetheless, a one-dimensional analysis may be in error because the flow must pass through zones of low conductivity that would normally be circumvented in three-dimensional flow.

If flow occurs primarily through macropores and the interlift zone, however, a one-dimensional analysis will not suffice. Liquid must be able to travel vertically through macropores within the lifts and horizontally in the interlift zones. The nature of the discrete flow field requires that a multidimensional analysis be performed.

Two models are presented in this paper: one-dimensional flow in a continuum and multidimensional flow through macropores. Indeed, soil liners probably exhibit characteristics expected of both models, but difficulties prevent modeling both types of flow concurrently. It is expected that these models serve to bracket the actual behavior of soil liners.

SPATIAL VARIABILITY OF HYDRAULIC PROPERTIES

The hydraulic properties of compacted soil are spatially variable and can fluctuate significantly within short distances. For example, Fig. 3 shows hydraulic conductivity measurements obtained by Rogowski (1990) on a large test pad of compacted clay constructed with three lifts that were 10 cm thick. The pad was partitioned into 250 squares (1 m × 1 m), ponded with water, and outflow from drains beneath the squares was measured. Hydraulic conductivities, determined from the outflow measurements of each square, are shown in Fig. 3. It is evident from Fig. 3 that significant fluctuations in hydraulic conductivity exist in compacted soil. As a result of these fluctuations, the hydraulic conductivity at any point in a soil liner is subject to uncertainty.

Deterministic hydraulic analyses of spatially variable soil do not account for uncertainty in a rigorous manner. By stochastic modeling, however, incomplete knowledge of the hydraulic properties of soil and the uncertainty associated with these properties can be mathematically incorporated into an analysis. Analyses of soil properties (Vanmarcke 1977a), slope stability

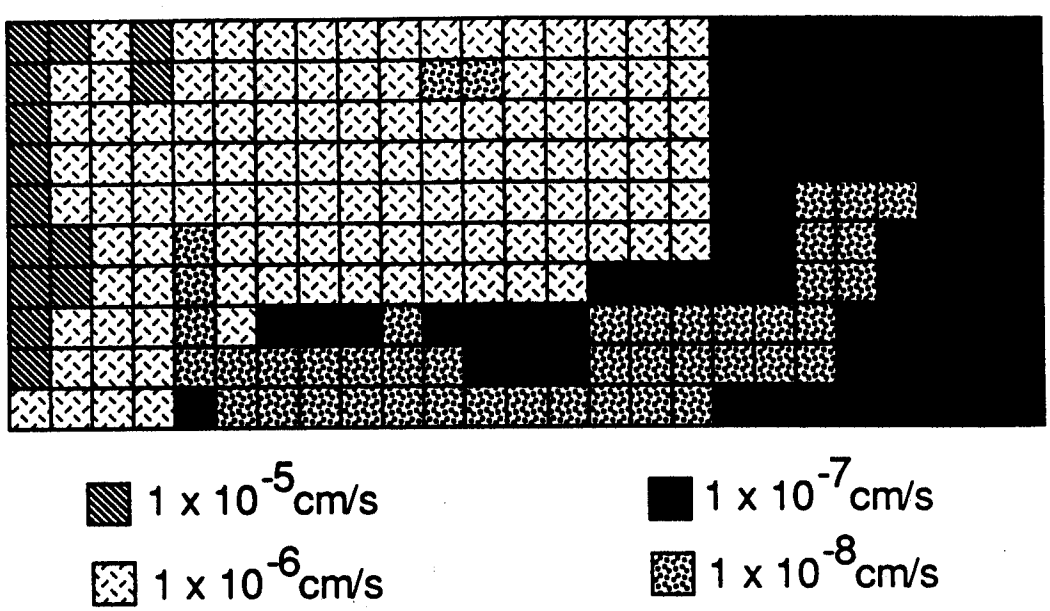

FIG. 3. Measurements of Hydraulic Conductivity on Test Pad [from Rogowski (1990)]

(Catalán and Cornell 1976; Vanmarcke 1977b), dissipation of pore pressures during consolidation (Hachich and Vanmarcke 1984), and foundation stability (Wu and Kraft 1967; Ronold 1990a, b) in spatially variable soils have been successfully performed using stochastic methods. In the present paper, stochastic models are used to describe how uncertainty and spatial variability of compacted soil affect flow in soil liners.

ONE-DIMENSIONAL CONTINUUM MODEL

Fig. 4 depicts a vertical section of a soil liner covered with liquid to depth H_L that is simulated with the one-dimensional model. The section of soil is composed of N lifts of thickness L_i and the hydraulic conductivity K_i is a random variable that varies spatially within each lift. The soil liner is assumed to consist of numerous vertical sections that are similar to the section in Fig. 4, but each section is described by a random, independent set of hydraulic conductivities. Hence, Fig. 4 represents a single realization of a vertical profile at a particular point in the soil liner.

Hydraulic Formulation

In this analysis, the following assumptions have been made: (1) The soil is initially saturated with an average equivalent, saturated hydraulic conductivity ($\bar{K}_{eq}$); (2) the liquid is placed upon the liner instantaneously; (3) the depth of liquid covering the liner remains constant; (4) the flow is steady and one dimensional; (5) the liquid does not affect the hydraulic conductivity of the soil; and (6) there is no suction at the base of the liner. These assumptions are admittedly idealized, but simplifications are necessary to render the analysis tractable. For soil liners compacted wet of optimum, however, the degree of saturation is generally in the range of 80–95%. Hence, the assumption of steady, saturated flow is reasonable for soils compacted wet of optimum.

Under these assumptions, the equivalent hydraulic conductivity K_{eq} of a vertical section through the liner can be written as a function of the hydraulic conductivities K_i and thicknesses of the lifts L_i

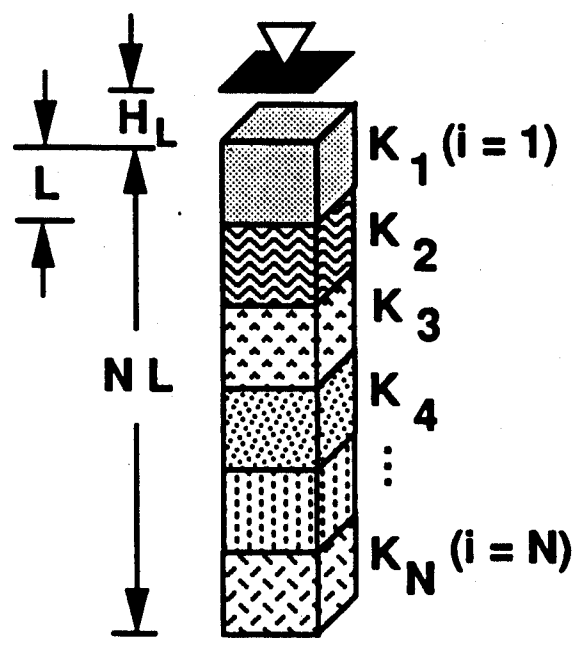

FIG. 4. Random Vertical Section of Soil Liner in Continuum Model

$$K_{eq} = \frac{\sum_{i=1}^{N} L_i}{\sum_{i=1}^{N} \frac{L_i}{K_i}} \quad \ldots\ldots (1)$$

It should be noted that K_{eq} is the harmonic mean of the hydraulic conductivities of the lifts.

The flux V_f is obtained by combining Darcy's Law with (1). Flux is defined here as flow rate per unit area. Darcy's law, for the section of the liner shown in Fig. 4, can be written as

$$V_f = K_{eq} \left(\frac{H_L + \sum_{i=1}^{N} L_i}{\sum_{i=1}^{N} L_i} \right) \quad \ldots\ldots (2)$$

where the term in parentheses is equal to the hydraulic gradient. If the lifts are assumed to be of equal thickness (i.e., $L_i = L$), the flux can be written as:

$$V_f = \frac{H_L + NL}{L} \left(\sum_{i=1}^{N} \frac{1}{K_i} \right)^{-1} \quad \ldots\ldots (3)$$

The seepage velocity V_s can be approximated by dividing the flux by the effective porosity n_e to account for the actual cross-sectional area of flow

$$V_s = \frac{V_f}{n_e} = \frac{H_L + NL}{Ln_e} \left(\sum_{i=1}^{N} \frac{1}{K_i} \right)^{-1} \quad \ldots\ldots (4)$$

where effective porosity is defined as the volume of voids that are effective in conducting flow divided by the total volume of the soil. Hence, the first-passage time T for plug flow is

$$T = \frac{NL^2 n_e}{H_L + NL} \left(\sum_{i=1}^{N} \frac{1}{K_i} \right) \quad \ldots\ldots (5)$$

Each variable in (3) and (5) involve some type of uncertainty. Thus, the first-passage time T and flux V_f are inherently random variables and their probability distributions are functions of the distributions of the independent variables in (3) and (5). Of all the independent variables, however, the hydraulic conductivity is most significant because it can fluctuate several orders of magnitude whereas fluctuations of the other variables are generally much smaller. Hence, it is assumed that only hydraulic conductivity is a random variable.

To simplify the analysis, hydraulic resistivity R_i is defined as the reciprocal of hydraulic conductivity at a point in a lift. If hydraulic resistivity is assumed to be random and the thickness of the lifts and effective porosity are assumed to be spatially homogeneous and deterministic, (3) and (5) can be simplified into linear combinations of hydraulic resistivity

$$V_f = \eta_1 \left(\sum_{i=1}^{N} R_i \right)^{-1} \quad \ldots\ldots (6)$$

and

$$T = \eta_2 \sum_{i=1}^{N} R_i \quad \text{(7)}$$

where η_1 and η_2 = deterministic coefficients

$$\eta_1 = \frac{H_L + NL}{L}; \qquad \eta_2 = \frac{n_e NL^2}{H_L + NL} \quad \text{(8)}$$

Stochastic Formulation

Probability Distribution of Hydraulic Conductivity and Resistivity

Hydraulic conductivity is often assumed to be lognormally distributed (Benson 1989; Johnson et al. 1990, Bogardi et al. 1989; Krapac et al. 1989; Richards and Thompson 1989). The validity of this assumption can be analyzed statistically (Freeze 1975) and is illustrated by the histograms of Rogowski's (1990) data shown in Fig. 5. For example, Fig. 5(*a*) is a histogram of Rogowski's (1990) data after trends in the mean (i.e. the trend of decreasing hydraulic conductivity from upper left to lower right exhibited in Fig. 3) and variance were removed by filtering. Fig. 5(*b*) is a histogram of the logarithms of the data. As shown by the normal density function fitted to the data [Fig. 5(*b*)], the normal distribution reasonably describes the logarithms of Rogowski's (1990) measurements of hydraulic conductivity. Hence, Rogowski's (1990) measurements can be described by the lognormal distribution.

The lognormal distribution has the density function

$$f_K(k) = \frac{1}{\sqrt{2\pi}\sigma k} \exp\left[-\frac{1}{2}\left(\frac{\ln k - \mu}{\sigma}\right)^2\right] \quad \text{(9)}$$

where the parameters μ and σ^2 are the log mean and the log variance, respectively. Since hydraulic conductivity is assumed to be lognormal with parameters μ and σ^2, hydraulic resistivity is also lognormal, but with parameters $-\mu$ and σ^2 (Aitchison and Brown 1957).

Transformation to First-Passage Time and Flux

Eqs. (6) and (7) state that the first-passage time and flux are functions of the summation of the hydraulic resistivities. Because each lift of soil is constructed independently, it is plausible to assume that the spatial distribution of resistivity in each lift is stochastically independent of the distributions of resistivity in the other lifts. If Z is defined as the summation of resistivities

$$Z = \sum_{i=1}^{N} R_i \quad \text{(10)}$$

then, by independence, the probability density function of Z, $f_Z(z)$, is the $(N - 1)$-fold convolution integral (Grimmett and Stirzaker 1982)

$$f_Z(z) = \int_0^\infty \int_0^\infty \cdots \int_0^\infty f_{R_N}(z_{N-1} - z_{N-2}) f_{R_{N-1}}(z_{N-2} - z_{N-3})$$

$$\cdots f_{R_2}(z_1 - r_1) f_{R_1}(r_1)\, dr_1\, dz_1\, dz_2 \cdots dz_{N-1} \quad \text{(11)}$$

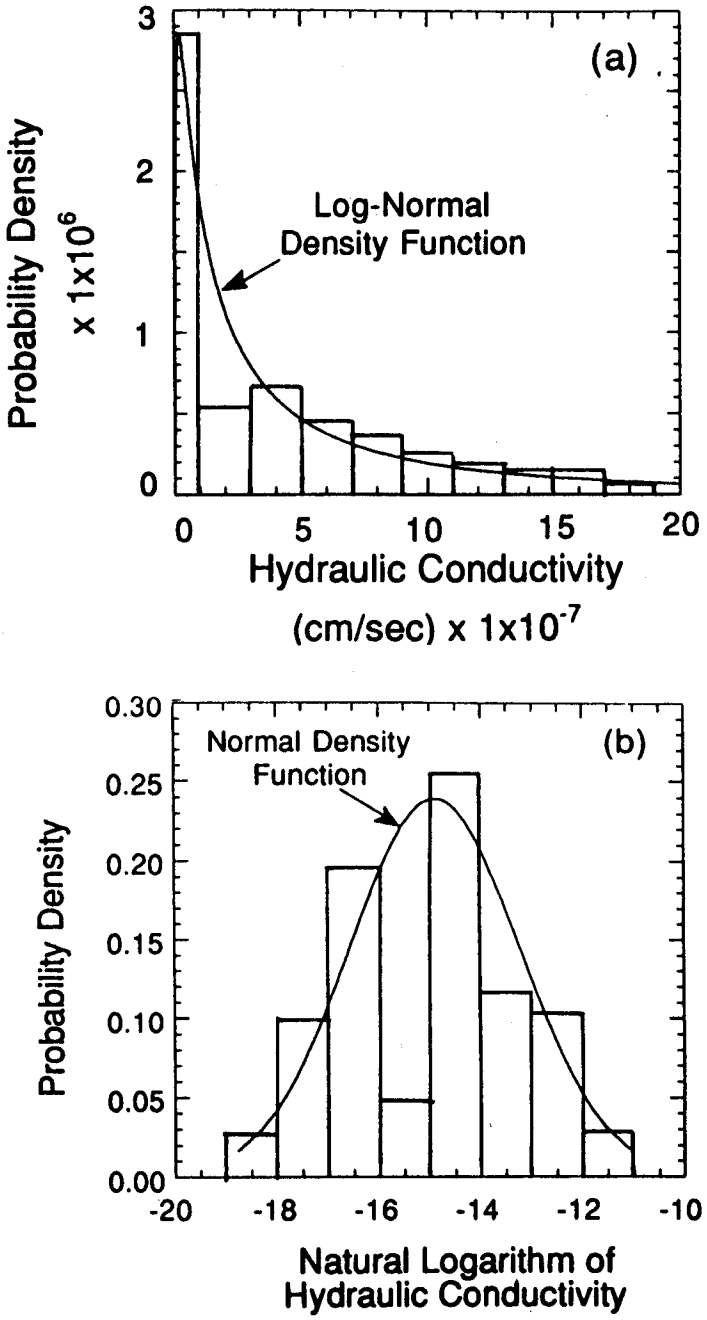

FIG. 5. Histograms and Density Functions of: (*a*) Hydraulic Conductivity; (*b*) Log-Hydraulic Conductivity

where Z_i is the sum of the first $i + 1$ resistivities (i.e., $Z_1 = R_1 + R_2$, $Z_2 = R_1 + R_2 + R_3$, etc.).

The probability density function $f_Z(z)$ can be determined by performing the integration shown in (11). It is easier, however, to determine $f_Z(z)$ by exploiting the Fourier convolution theorem. The Fourier convolution theorem states that the Fourier transform of an $(N - 1)$-fold convolution integral, $\Phi_z(\xi)$, is the N-times product of the Fourier transformations of the integral's arguments, $\Phi_i(\xi)$ (Churchill 1972). Hence, the Fourier transform of (11) can be written as

$$\Phi_z(\xi) = \prod_{i=1}^{N} \Phi_{R_i}(\xi) \quad \ldots\ldots\ldots\ldots\ldots\ldots\ldots\ldots\ldots\ldots\ldots\ldots \quad (12)$$

where

$$\Phi_{Ri}(\xi) = \int_{-\infty}^{\infty} f_{Ri}(r)e^{-i\xi r}\, dr \quad \text{(13)}$$

is the Fourier transform of the density function of hydraulic resistivity. The Fourier transform $\Phi_R(\xi)$, is also known as the characteristic function of R.

If the hydraulic resistivities are assumed to be identically distributed, which is plausible unless the soil or construction method vary from lift to lift, (13) becomes (Grimmett and Stirzaker 1982)

$$\Phi_z(\xi) = [\Phi_{Ri}(\xi)]^N \quad \text{(14)}$$

To obtain $f_Z(z)$, the Fourier inversion of $\Phi_z(\xi)$ is performed

$$f_Z(z) = \int_{-\infty}^{\infty} \Phi_Z(\xi)e^{i\xi z}\, d\xi \quad \text{(15)}$$

The density functions of the first-passage time $f_T(t)$ and flux $f_F(f)$ are obtained from $f_Z(z)$ by probability integral transform (Grimmett and Stirzaker 1982). The relationships of $f_T(t)$ and $f_F(f)$ to $f_Z(z)$ are

$$f_F(f) = \frac{\eta_1}{f^2} f_z\left(\frac{\eta_1}{f}\right) \quad \text{(16)}$$

$$f_T(t) = \frac{1}{\eta_2} f_z\left(\frac{t}{\eta_2}\right) \quad \text{(17)}$$

Numerical Integration

Unfortunately, a closed-form solution for the Fourier transform of a lognormal density function cannot be obtained. Thus, the Fourier integrals must be performed numerically. Several numerical methods were investigated as means to perform the integration; the fast Fourier transform (Press et al. 1986) proved to be the simplest method to implement and provided the most stable solutions (Benson 1989).

Comparison of Numerical Results with Monte Carlo Simulation

To verify the numerical solution, the distributions of flux and first-passage time have been compared to results obtained by Monte Carlo simulation. The numerical procedure was used for all analyses described in the present paper, however, because it is computationally efficient and provides precise results, even in the tails. To perform the simulation, hydraulic resistivities were randomly sampled from a lognormal distribution and the flux and first-passage time were computed from (6) and (8). The sampling procedure was repeated 800 times to obtain a sufficient number of realizations of V_f or T to represent the distributions. The parameters used in the analysis presented herein are $\mu = -17$, $\sigma^2 = 1.0$, $N = 6$, $L = 15$ cm, $H_L = 30$ cm, and $n_e = 0.40$.

Fig. 6 is a comparison of analytic and Monte Carlo results for first-passage time. The graph shows the reliability function $R_T(t)$ obtained by the method outlined in (7)–(13), and the reliability function estimated by Monte Carlo simulation. The reliability function yields the probability that the first-passage time T exceeds a time t

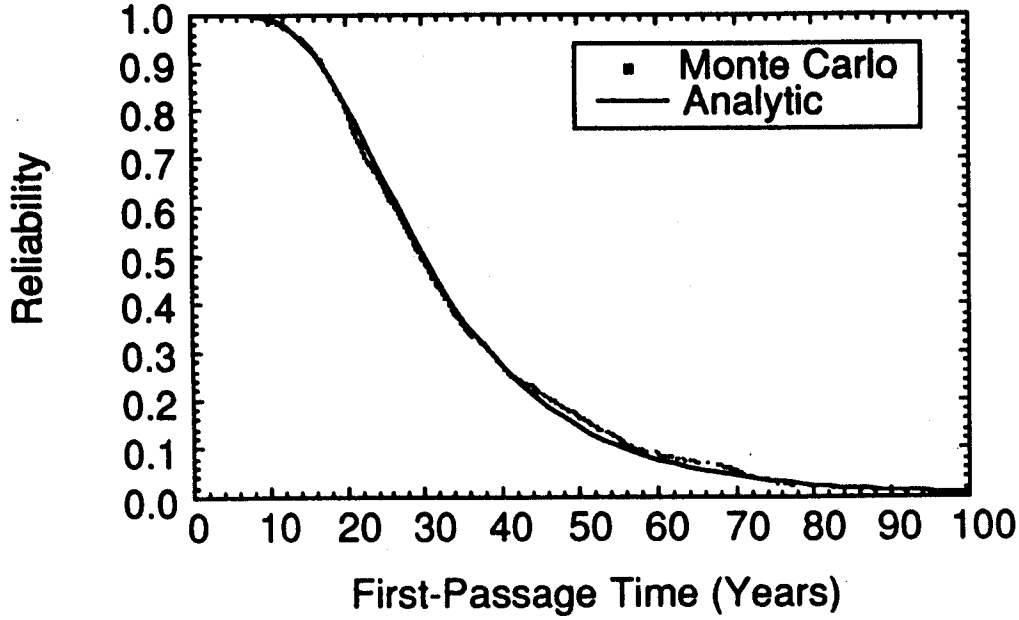

FIG. 6. Comparison of Analytic Solution and Monte Carlo Simulation of Reliability Function for One-Dimensional Continuum Model

$$R_T(t) = \int_t^{\infty} f_T(t)\, dt = P(T \geq t) \quad \ldots\ldots\ldots\ldots\ldots\ldots\ldots\ldots \quad (18)$$

As shown in Fig. 6, the reliability functions obtained by the analytic procedure and simulation are similar, even in the tails of the distributions. Comparisons made for different thicknesses (N = 1–20) and with other parameters (μ = −11 to −20, σ^2 = 0.1–2.5) agreed equally well. The numerical procedure was also examined to be sure the first-passage time converged to the deterministic condition as the coefficient of variation of hydraulic conductivity approached zero.

THREE-DIMENSIONAL MACROPORE MODEL

A schematic representation of the soil liner being analyzed by the three-dimensional model is shown in Fig. 7. The analysis is performed on a cross-sectional area of the liner A sufficiently large to adequately incorporate variability. The liner is assumed to be composed of N lifts of thickness L and between each lift is a planar region of thickness b that represents the interlift zone. Each lift is divided into N_p equal-sized square partitions that are perforated by vertically oriented cylindrical channels that represent macropores. Flow is assumed to occur only in the channels and the interlift zones; hence, the matrix of the soil is assumed to be impervious.

To simplify the analysis, only saturated flow was considered. Often times the formation of macropores is associated with soil liners compacted dry of optimum where the degree of saturation may be less than 80%. Under these unsaturated conditions, significant suctions may be present and the unsaturated hydraulic conductivity will be lower than expected under saturated conditions. These effects are ignored by assuming the soil is saturated. However, the combined effects of suction (which increases the hydraulic gradient) and lower hydraulic conductivity tend to compensate each other when combined in Darcy's law. As a result, the rate of flow in unsaturated and saturated liners may not be substantially different. Nevertheless, with-

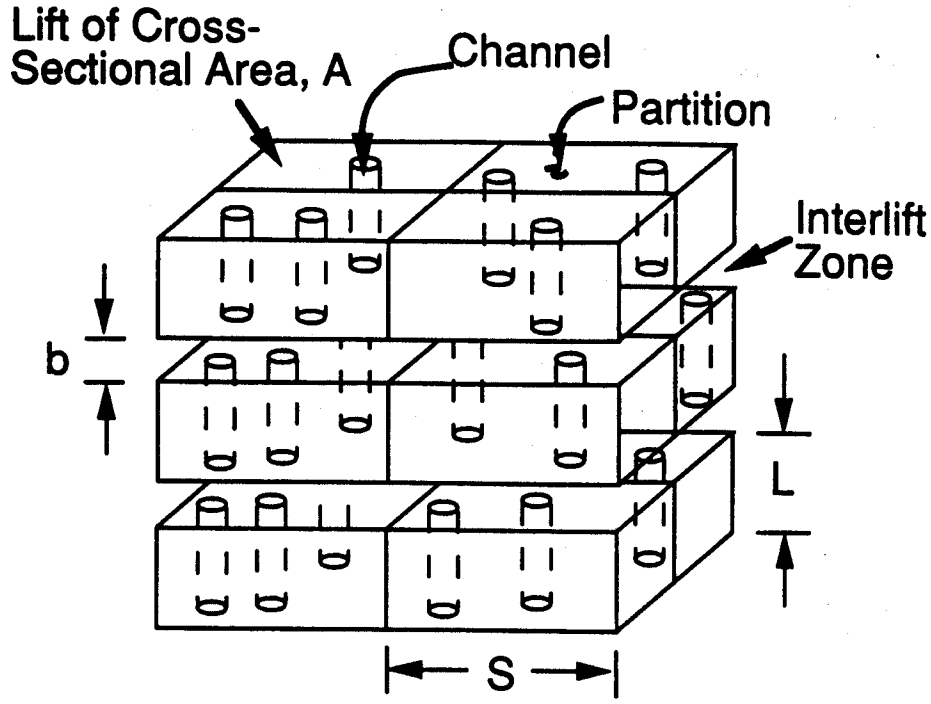

FIG. 7. Soil Liner Modeled with Three-Dimensional Macropore Model

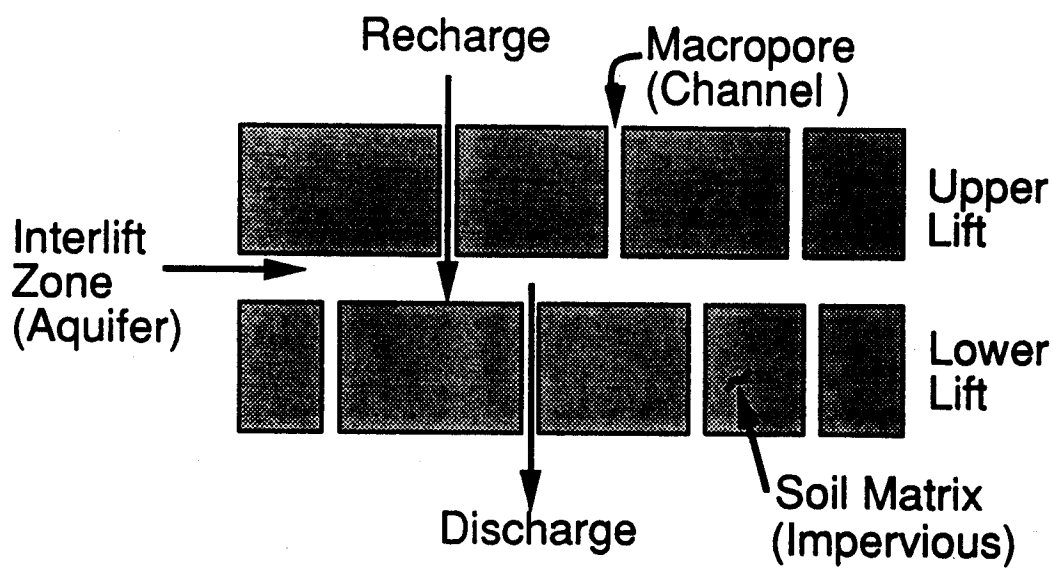

FIG. 8. Hydraulic Behavior of Interlift Zone

out a more detailed analysis, it is difficult to determine how unsaturated conditions will affect the first-passage time. In the long-term condition, however, the liner will eventually become saturated. Hence the results regarding flux (or equivalent hydraulic conductivity) should not be affected by the assumption of saturation.

Hydraulic Formulation

To determine the distributions of first-passage time and flux, a hydraulic model must be formulated that relates the properties of the liner to the properties of the flow field. The interlift zone, shown in Fig. 8, is assumed to behave as a confined aquifer subjected to injection wells (channels above

the interlift zone) and discharge wells (channels below the interlift zone). A linear flow equation is used to compute the flow rate Q_j for each channel. For the jth channel, Q_j is

$$Q_j = J_j(h_{1j} - h_{2j}) \quad \text{(19)}$$

where J_j = flow coefficient of channel j; h_{1j} = total hydraulic head at the top of channel j; and h_{2j} = total hydraulic head at the bottom of channel j. To ensure the flow was laminar, Reynolds numbers were checked and were found to be far below critical values (≈2,000) for the transition to turbulence (Streeter and Wiley 1978). A discussion of the method to determine J_j is described in a later section.

The Theim equation for radial flow in a confined aquifer is used to determine the hydraulic head H_{ik} at any point k in the ith interlift zone

$$H_{ik} = \frac{1}{2\pi T_r^{(i)}} \sum_{j=1}^{N_i} Q_j \ln(r_{jk}) + W_i \quad \text{(20)}$$

where N_i = number of channels that interact with the ith interlift zone; H_{ik} = hydraulic head at any point k in the ith interlift zone; r_{jk} = radial distance between point k and jth channel; $T_r^{(i)}$ = transmissivity of the ith interlift zone; and W_i = a constant. When the point k coincides with the location of channel j, r_{jk} is taken as r_j, the radius of the channel.

Although the Theim equation is commonly used for radial flow to a well located in a porous medium, in this analysis it describes flow in a planar zone between lifts (Fig. 7). This application is valid because the Theim equation is derived by integrating the Laplace equation and applying boundary conditions corresponding to laminar flow in a cylindrical control volume with a point source at its center. In this capacity, however, transmissivity is actually a laminar flow coefficient for flow in the planar zone rather than a hydrogeologic variable corresponding to flow through porous media.

Substitution of (19) into (20) yields

$$H_{ik} = \frac{1}{2\pi T_r^{(i)}} \sum_{1}^{N} J_j(h_{1j} - h_{2j})\ln(r_{jk}) + W_i \quad \text{(21)}$$

which is written for each channel in each interlift zone.

To ensure conservation of mass, continuity equations are written for each interlift zone that require all flow into an interlift zone to leave the interlift zone

$$\left(\sum_{1}^{N_{in}} Q_j\right)_{in} = \left(\sum_{1}^{N_{out}} Q_j\right)_{out} \quad \text{(22)}$$

Substitution of (19) into (22) yields

$$\left[\sum_{1}^{N_{in}} J_j(h_{1j} - h_{2j})\right]_{in} = \left[\sum_{1}^{N_{out}} J_j(h_{1j} - h_{2j})\right]_{out} \quad \text{(23)}$$

which is written for each interlift zone.

The hydraulic problem is solved by computing the heads at the end of each channel and the constants W_i for each interlift zone. In hydrogeologic practice, W_i is normally specified as the undisturbed hydraulic head far from the well. In this analysis, W_i serves a similar function, but it is solved for directly when the solution for the heads is obtained. Eq. (21) is written for

both ends of each channel where the location i in (21) corresponds to the center of the channel. This set of equations is combined with the continuity equations, (23) written for each interlift zone to form a linear system of equations of the form

$$\mathbf{AH} = \mathbf{C} \quad \text{(24)}$$

The matrix **A** consists of coefficients that multiply the hydraulic heads and the constants W_i. The vector **H** is composed of the unknown hydraulic head at the end of each channel and the unknown constants W_i. Boundary conditions and zeros comprise the vector **C**. To solve for the heads, (24) is inverted to obtain the head vector **H**.

First-Passage Time, Flux, and Tortuosity

First-Passage Time

The first-passage time T for a particular realization is computed by determining the minimum time of travel through all possible pathways that penetrate the entire thickness of the liner. To obtain the time of travel for each path, the time of travel in the channels and the interlift zones is computed and added. The time of travel within the jth channel t_j is computed by combining (19), the radius of the channel r_j, and the thickness of a lift L

$$t_j = \frac{L\pi r_j^2}{J_j(h_{1j} - h_{2j})} \quad \text{(25)}$$

A similar expression yields an approximate time of travel in the interlift zone t_{jk} between channels j and k in the upper and lower adjacent lifts

$$t_{jk} = \frac{d_{jk}^2 b}{T_r(h_{2j} - h_{1k})} \quad \text{(26)}$$

where d_{jk} = radial distance between channels j and k. Eq. (26) is a direct application of Darcy's law and is exact only if the hydraulic gradient is directed from channel j to channel k; otherwise, it yields a time of travel that is too short. Hence, the approximation is conservative. Furthermore, because the transmissivity is a flow coefficient for flow in the planar interlift zone and not a porous medium, a porosity term is not included in (26).

Eq. (26) was used to avoid implementing a complex algorithm to find the exact flow path in interlift zones that have highly nonlinear fields of hydraulic head. No attempt was made, however, to evaluate the error of the approximation. Even with the approximation, execution times were very long (>15 h) because of the recursive algorithm required to find the path with shortest time of travel. An exact analysis would require implementing an algorithm for flow paths in each step of recursion and would increase execution times substantially.

Flux Emanating from Base of Liner

The flux that emanates from the base of the liner V_f is obtained by adding the flow rates of liquid exiting the channels in the bottom of the liner and dividing by the area A. The flux also can be interpreted in terms of an equivalent hydraulic conductivity K_{eq} by Darcy's law

$$K_{eq} = \frac{V_f}{I_{av}} \quad (27)$$

where I_{av} = average vertical hydraulic gradient.

Tortuosity

The tortuosity τ is the measure of the irregularity of the pathway of first passage and is defined as the length of the pathway of first passage, L_{fp}, divided by the thickness of the liner

$$\tau = \frac{L_{fp}}{NL} \quad (28)$$

where N = number of lifts. Tortuosity reflects the distance the liquid travels in the interlift zone. If the liquid flows only vertically downward (no horizontal flow in the interlift zone), the tortuosity is 1; if the liquid travels in the interlift zones, the tortuosity is greater than 1.

Stochastic Formulation

The hydraulic model formulated in the preceding section can be generically applied to any random realization of the soil liner shown in Fig. 7. To incorporate spatial variability, Monte Carlo simulation is used to transform the distributions of hydraulic properties to distributions of first-passage time, flux, and tortuosity. For each scenario, numerous random realizations of a soil liner are generated by randomly sampling the properties of the liner (e.g., size and location of the macropores) from their probability distributions. Then, the hydraulic behavior of the liner is analyzed as if the problem is deterministic. Results, such as the first-passage time and flux, are recorded for each realization and a statistical analysis is performed on the collection results when the simulation is complete. The probability distributions assigned to the properties of the liner are described in the following sections and are summarized in Table 1.

Number and Location of Channels

A truncated two-dimensional Poisson distribution was used to assign the number of channels N_c in each partition. Table 1 includes the density function of the truncated Poisson distribution and the densities of other distributions used to describe the soil liner. The selection of the Poisson distribution was arbitrary, but it is commonly used to describe events that occur independently in a span of time or region of space (Ang and Tang 1975).

The Poisson distribution has a finite probability of realizations of zero, but a realization of no channels in a partition implies that the partition cannot conduct flow. Realizations of no flow seem unlikely; hence, the Poisson distribution was truncated to eliminate realizations of zero. The probability mass associated with realizations of zero was added to realizations of one channel.

An underlying assumption of the Poisson distribution is that events, in this case the occurrence of channels, are uniformly distributed in space. In an actual soil liner, the macropores may be grouped in zones where the molding water content was too low or the compactive effort was insufficient to adequately deform clods and eliminate interclod voids. Nevertheless, since little is known about the statistical properties of macropores, a more complex scheme to distribute the channels seem unwarranted. Eq. (21),

TABLE 1. Assumed Distributions of Hydraulic Properties

Property (1)	Applicable model (2)	Assumed distribution (3)	Density function (4)
Hydraulic cond. of a partition, K	1-D and 3-D	Lognormal	$f_K(k) = \frac{1}{\sqrt{2\pi}\sigma k} \exp\left[-\frac{1}{2}\left(\frac{\ln k - \mu}{\sigma}\right)^2\right]$
Number of channels/partition, N_c	1-D	Truncated Poisson	$f_{N_c}(n) = 0, n = 0; f_{N_c}(n) = e^{-\lambda}(\lambda + 1), n = 1; f_{N_c}(n) = \frac{\lambda^n e^{-\lambda}}{n!}$
Location of channels (X, Y) in partition[a]	3-D	Uniform	$f_X(x) = \frac{1}{S}; f_Y(y) = \frac{1}{S}$
Cross-sectional area of channels in partition, A_c	3-D	Truncated normal $(A_c > 0)$	$f_{A_c}(a_c) = \frac{N_c}{\sqrt{2\pi}C_{VAC}n_eS^2} \exp\left[-\frac{1}{2}\left(\frac{N_a a_c - n_eS^2}{C_{VAC}n_eS^2}\right)^2\right]$
Transmissivity of interlift zone, T_r	3-D	Lognormal	$f_{T_r}(t) = \frac{1}{\sqrt{2\pi}\sigma_T t} \exp\left[-\frac{1}{2}\left(\frac{\ln t - \mu_{T_r}}{\sigma_{T_r}}\right)^2\right]$

[a]Partitions are square with dimensions $S \times S$.

however, requires that channels in the same or adjacent lifts not overlap. To avoid this inconsistency locations of the channels are constrained by assigning, from the uniform distribution, new locations for the overlapping channels.

Size of Channels

Little is known about the statistical properties of the size of macropores. Because of the lack of information, the cross-sectional area of macropores was related to the effective porosity that generally is normally distributed (Freeze 1975). The cross-sectional area of channels is linearly related to the effective porosity; i.e.

$$L \sum_{j=1}^{N_c} A_{cj} = LS^2 n_e \quad \text{(29)}$$

Normally distributed random variables are linearly reproductive. Hence, because A_{cj} is linearly related to n_e, A_{cj} was assumed to be normally distributed. Admittedly, this assumption is ad hoc, but virtually no data exists to describe the geometry of macropores and a reasonable technique was needed to account for variability in channel size.

To obtain the parameters of the distribution A_{cj}, the mean cross-sectional area $\bar{A}_c$ was related to the effective porosity by:

$$\bar{A}_c = \frac{S^2 n_e}{N_c} \quad \text{(30)}$$

A small coefficient of variation ($C_{VA_c} = 10$) was used to avoid realizations of very large or very small channels. For typical parameters used in the analyses (e.g., $n_e = 0.05$, $N_c = 100$ channels/m^2, $S = 20$ cm, and $L = 15$ cm; $C_{VA_c} = 10$), 95% of the macropores had a radius in the range of 0.6–0.9 cm.

Flow Coefficients

In this model, macropores are assumed to be vertically oriented cylindrical channels. One method to compute the flow coefficients of the channels (and the hydraulic conductivity of a partition) is to assume the channels are capillary tubes. Then, the flow coefficient can be computed from the Hagen-Poiseuille equation (Streeter and Wiley 1979):

$$J_j = \frac{Q_j}{\Delta H} = \frac{\mathrm{g} A_{cj}^2}{8\pi\nu L} \quad \text{(31)}$$

where ΔH = change in total head; g = gravimetric acceleration; and ν = kinematic viscosity of water.

Macropores, however, are not capillary tubes. Instead, the flow path through a macropore is tortuous and has continually varying aperture. A partition with several large macropores might have very small hydraulic conductivity if the aperture size of the macropores varied significantly and their path through the liner was tortuous. Conversely, a partition containing only one small macropore with smooth vertical walls may have very large hydraulic conductivity. Because (21) cannot account for these conditions, its use to calculate the flow coefficient may be inappropriate.

A simpler approach was used here. First, the hydraulic conductivity of a partition K_i was randomly sampled from a lognormal distribution. Then,

the total flow through the partition Q (based on the sampled hydraulic conductivity and Darcy's law) was equated to the sum of the flows through each channel in the partition. To compensate for reduced resistance in larger macropores, the portion of the total flow assigned to each macropore was weighted by the ratio of the squared cross-sectional area of a channel to the sum of the squared areas of the channels; i.e.

$$J_j = K_i S^2 \frac{A_{cj}^2}{L \sum_{j=1}^{N_c} A_{cj}^2} \quad \text{(32)}$$

In this way, larger macropores are weighted with larger flow coefficients using a weighting scheme similar to Poiseuille's equation, but the strict hydraulics of flow in a capillary tube are avoided. The writers believe that this approach permits a wider range of realizations that can occur in a soil with macropores.

Transmissivity of Interlift Zone

A lognormal distribution was assumed for the transmissivity of the interlift zone because transmissivity is linearly proportional to hydraulic conductivity and hence should exhibit a similar distribution. No direct data is currently available on interlift transmissivity, however, to verify this assumption.

Number of Realizations

The number of realizations required for sufficient accuracy was determined by ensuring the first four moments of first-passage time and flux were stable; i.e. the estimates of the moments did not change significantly with additional realizations. A sensitivity analysis revealed that 600 realizations were required before the first two moments stabilized, but 800 realizations were necessary for the fourth moment to become stable. To be conservative, 1,000 realizations were used for all analyses. Benson (1989) provides a comprehensive discussion of the stability of the moments.

Area of Analysis and Heterogeneity of Soil

The cross-sectional area of analysis A (Fig. 7) and the number of partitions N_p must be selected to satisfy three criteria: (1) adequate representation of three-dimensional heterogeneity; (2) adequate representation of distributions describing the channels; and (3) reasonable time to perform the simulation. To satisfy the first criterion, A must be large enough, and be divided into a sufficient number of partitions, to simulate three-dimensional heterogeneity. When A and N_p are increased to model heterogeneity, however, the second and third criteria may not be satisfied. Small increases in A yield large increases in the execution time required to complete a simulation and as N_p is made larger, the distributions that describe the channels are not preserved because partitions that are small have a probability of realizing one channel that is large. Hence, the number, location, size, and flow coefficients of channels will be improperly represented if N_p is large.

The effect of diminished representation of the distribution describing the channels is a limitation of the model caused by the assumption of flow that occurs only in the macropores and not in the soil matrix. Hence, a compromise must be made between A, N_p, and the execution time required to perform the simulation.

Cross-Sectional Area

To determine A that adequately represents heterogeneity, the sensitivity of the distributions of first-passage time T and flux F distributions were examined by graphing the sample mean, $\bar{T}$ or $\bar{V}_f$, and variance, Var(T) or Var(V_f), as a function of A. Fig. 9 shows the sensitivity of these statistics for a mean number of channels/m^2, λ, of 45, 100, and 175, and N_p of 4. The graphs show that the distributions are sensitive to A; T and Var(V_f) become larger and $\bar{V}_f$ and Var(V_f) become smaller. Nevertheless, the changes in the distributions become small when A exceeds 1,500 cm^2 and the sensitivity to area is less pronounced when λ becomes larger. Hence, A of 1,500 cm^2 was selected for use in subsequent analyses of sensitivity. For A of 1,500 cm^2, a typical simulation required nearly 15 h to execute on a high-speed personal computer. When the area was increased to 2,500 cm^2, the execution times rose to 48 h.

Number of Partitions

The number of partitions to be used in subsequent sensitivity analyses was also identified by examining the sensitivity of T and V_f to N_p. It was found that for N_p of 4, three-dimensional heterogeneity was preserved and the probability of zero channels per partition was small (Benson, 1989). Hence, N_p of 4 was selected for sensitivity analyses.

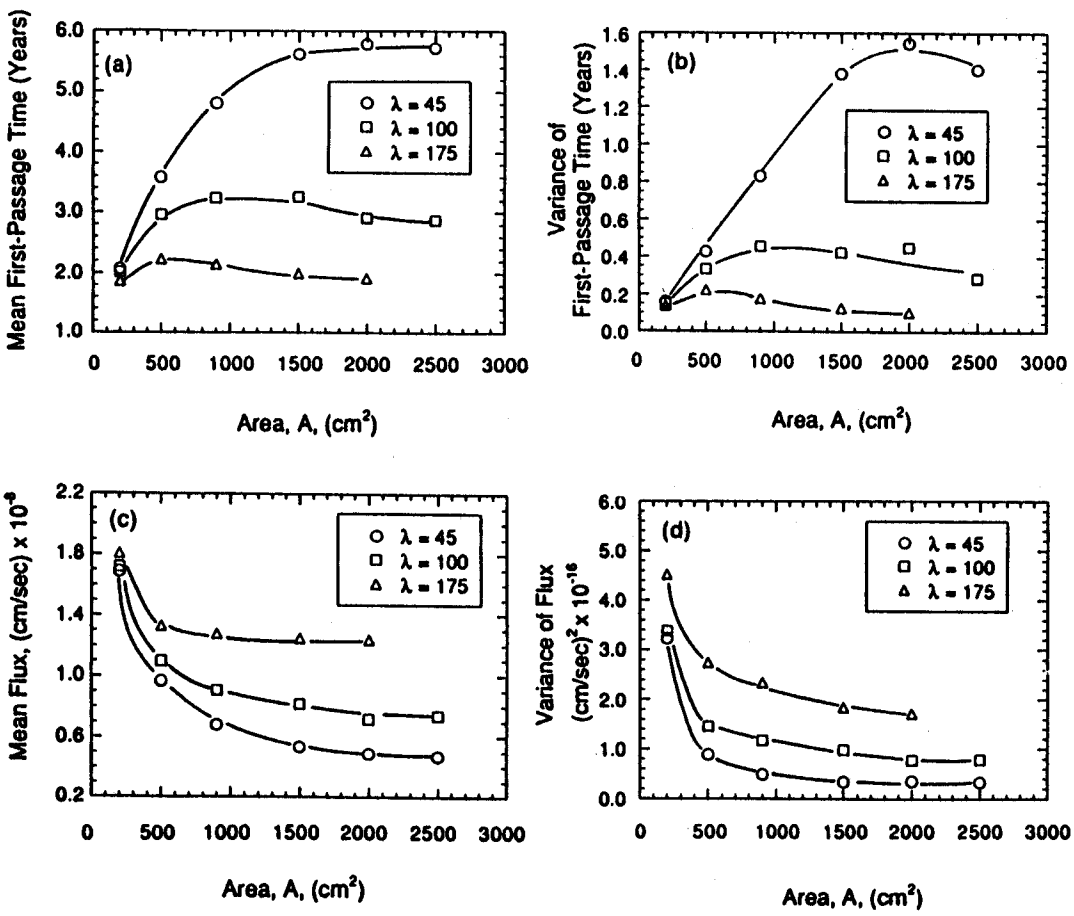

FIG. 9. Sensitivity of: (*a*) Mean First-Passage Time; (*b*) Variance of First-Passage Time; (*c*) Mean Flux; (*d*) Variance of Flux to Cross-Sectional Area *A*

Evaluation

It is nearly impossible to verify a stochastic model. It is possible, however, to evaluate whether the results of the model are consistent with expected behavior. To check for consistency, the characteristics of the distributions of first-passage time and flux were examined under various conditions.

First-Passage Time, Flux, and Transmissivity of Interlift Zone

The performance of a soil liner dominated by flow in macropores depends on the ability for liquid to flow in the interlift zone. If the transmissivity of the interlift zone is low, large amounts of energy will be dissipated as the liquid flows between the lifts. Furthermore, the likelihood is small that liquid will circumvent zones of low conductivity in the lifts by traveling a great distance in the interlift zone. Instead, the liquid will travel downward in pathways of lower conductivity that require a smaller expenditure of energy. Hence, the first-passage time will be large, the flux small, and equivalent hydraulic conductivity will be smaller than the mean hydraulic conductivity of a single lift.

Conversely, if the transmissivity of the interlift zone is high, the liquid will flow readily in the interlift zone and will travel far to reach favorable zones of high conductivity. Hence, when the transmissivity is large, regions in the lifts that have low conductivity become less important. Furthermore, the first-passage time will be short, the flux will be large, and the equivalent hydraulic conductivity will reach the mean hydraulic conductivity of a single lift.

To determine if the model would yield this expected behavior, the sensitivity to mean interlift transmissivity $\bar{T}_r$ was evaluated. Parameters for input were: mean hydraulic conductivity $\bar{K} = 5 \times 10^{-7}$ cm/s; coefficient of variation of hydraulic conductivity $C_{VK} = 150$; coefficient of variation of interlift transmissivity $C_{VT_r} = 0$; $N_p = 4$; mean number of channels $\lambda =$ 100 channels/m^2; $C_{V\Lambda_c} = 0$; $n_e = 0.05$; $N = 6$; $H_L = 30$ cm; $L = 15$ cm;

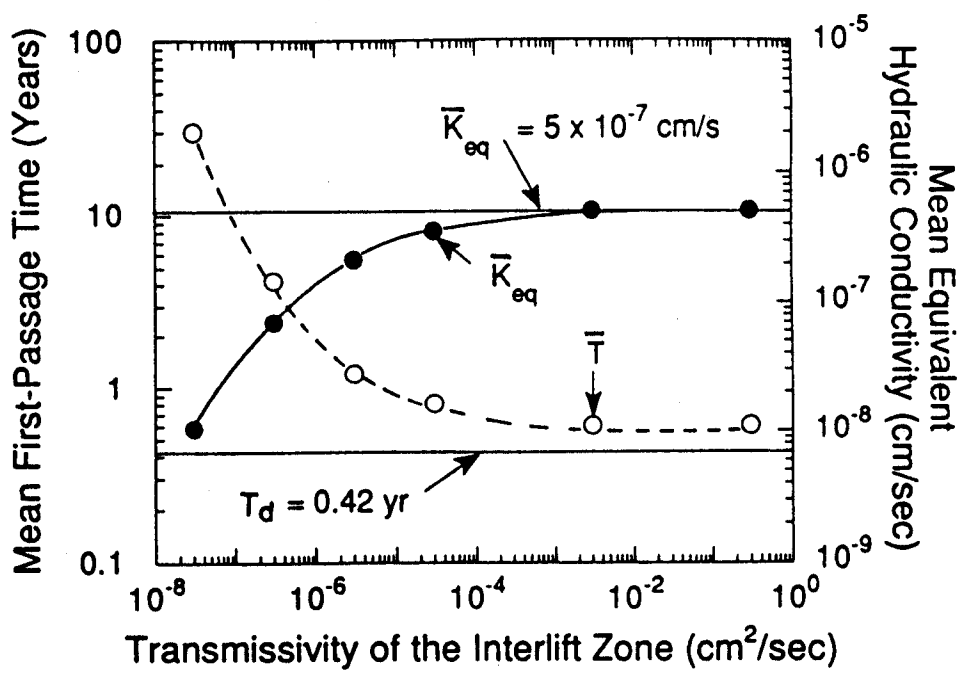

FIG. 10. Mean First-Passage Time and Mean Equivalent Hydraulic Conductivity as Function of Transmissivity of Interlift Zone

and $b = 3$ cm. The mean transmissivity was varied from 3×10^{-8} cm²/s to 0.3 cm²/s. Fig. 10 is a graph of mean first-passage time and mean equivalent hydraulic conductivity as a function of transmissivity of the interlift zone. The lower solid line corresponds to the time of travel for deterministic flow T_d computed with from Darcy's law and corrected for the irregularity of the flow path by multiplying by the square of mean tortuosity; i.e.

$$T_d = \frac{(NL\bar{\tau})^2 n_e}{\bar{K}(H_L + NL)} \quad \text{(33)}$$

where $\bar{\tau}$ is the mean tortuosity, (28), which was equal to 1.4. Fig. 10 shows the expected result; as the transmissivity becomes larger, the mean first-passage time decreases and approaches T_d.

A similar result is shown in Fig. 10 with regard to the mean equivalent conductivity $\bar{K}_{eq}$. A correction for length of the flow path was also applied to compute $\bar{K}_{eq}$; i.e.

$$\bar{K}_{eq} = \frac{\bar{V}_f}{I^*} = \frac{\bar{V}_f}{\left(\dfrac{H_L + NL}{NL\bar{\tau}}\right)} \quad \text{(34)}$$

where I^* = hydraulic gradient corrected for tortuosity. Fig. 10 shows that $\bar{K}_{eq}$ rises as the transmissivity increases and reaches the mean hydraulic conductivity of a lift (5×10^{-7} cm/s, the upper solid line) when the transmissivity is large.

Convergence to Deterministic Case

An additional check for consistency was conducted by removing the variability in hydraulic conductivity, transmissivity of the interlift zone, and area of the channels. The variability in number and location of the channels, however, could not be removed because the Poisson distribution is used to describe the number of channels. The same input parameters used to evaluate sensitivity to $\bar{T}_r$ were used to evaluate convergence, except C_{VK} was varied from 0–200 and $\bar{T}_r$ was fixed at 0.3 cm²/s to eliminate the influence of the interlift zone.

Fig. 11 shows the coefficient of variation of first-passage time C_{VT} and the coefficient of variation of flux C_{VF} as a function of C_{VK}. As C_{VK} is reduced, C_{VT} and C_{VV_f} become smaller. When C_{VK} is zero, C_{VT} is small but not zero because the first-passage time depends on the number and location of the channels in each lift (defined by the Poisson distribution) from which the variability cannot be removed. Unlike C_{VT}, $C_{VV_f} = 0$ when $C_{VK} = 0$, which is exactly the result that is expected.

SUMMARY OF ASSUMPTIONS AND FORMULATION

Two models of flow in compacted soil liners have been presented in this paper. One model considers one-dimensional flow through a series of horizontal lifts and in each lift the hydraulic conductivity is assumed to vary spatially. The other model simulates flow through a network of vertical macropores that are interconnected by planar interlift zones. The soil is assumed to be saturated in both models.

The primary assumptions used in the formulation of the one-dimensional model were: (1) The soil is initially saturated with an average equivalent, saturated hydraulic conductivity $\bar{K}_{eq}$; (2) the liquid is placed upon the liner

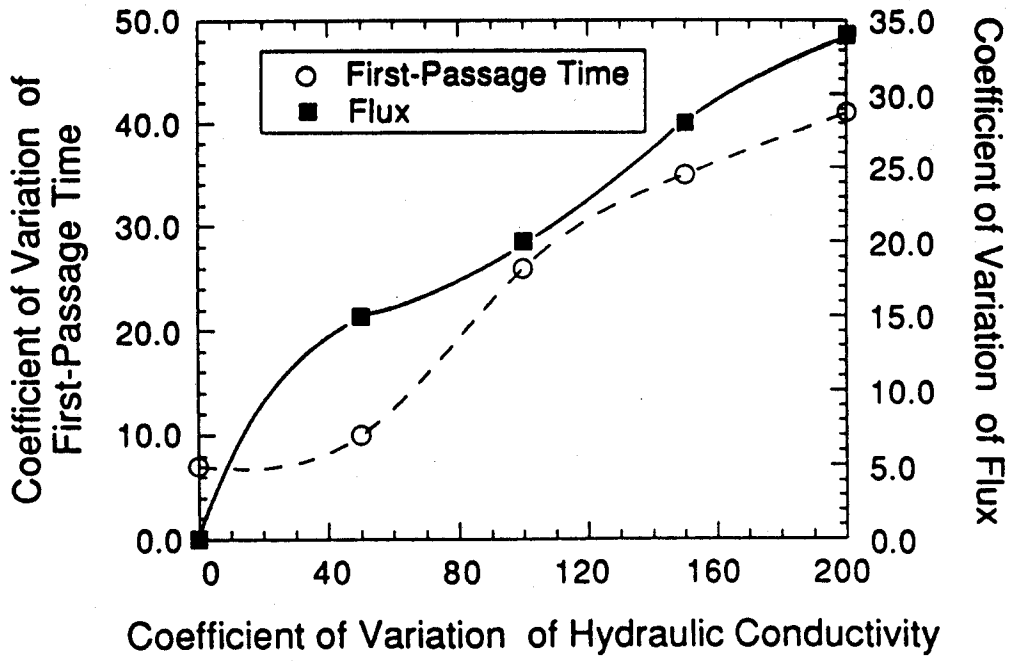

FIG. 11. Coefficient of Variation of First-Passage Time and Flux as Function of Coefficient of Variation of Hydraulic Conductivity

instantaneously; (3) the depth of liquid covering the liner remains constant; (4) the flow is steady and one dimensional; (5) the liquid does not affect the hydraulic conductivity of the soil, (6) there is no suction at the base of the liner, and (7) the distribution of hydraulic within each lift is lognormal and is not spatially correlated to the distribution of hydraulic conductivity in the other lifts. Standard equations for one-dimensional vertical flow through horizontal layers were used to determine the first-passage time and flux and characteristic equations were used to determine distributions for first-passage time and flux from the distribution of hydraulic conductivity. The Fourier integrals used to obtain the characteristic functions were performed numerically.

Flow in the macropore model is assumed to only occur in vertical cylindrical channels and in a planar zone between each lift. Because actual macropores vary in aperture, orientation, and shape (and hence are not smooth straight channels), the Poiseuille equation is not used to determine flow coefficients for the channels. Instead, the coefficients are assigned by requiring the sum of flows in all channels in a partition to equal the flow through the partition based on a randomly assigned hydraulic conductivity which is not correlated to the number of channels. The flow coefficients are also weighted by their cross-sectional areas (i.e. bigger channels have larger flow coefficients).

Heads in the planar interlift zone were computed using the Theim equation for radial flow in a confined aquifer. Channels in adjacent lifts are assumed to be injection and discharge wells. The interlift zone is assumed to be a planar zone of laminar flow. Thus, the transmissivity term in the Theim equation is essentially a laminar flow coefficient rather than a hydrogeologic parameter.

First-passage time in the macropore model is obtained by computing the time of travel in all pathways and then searching for the shortest time of travel. To simplify the analysis and enhance computational efficiency, time of travel in the interlift zone is computed by a direct application of Darcy's

law between the channels. This assumption yields travel times that are too short and hence is conservative.

To simulate spatial variability, probability distributions were assigned to describe the properties of the channels and interlift zones and Monte Carlo simulation was used to randomly sample variates from the distributions. Several of the distributions had to be assigned arbitrarily because little data is available to describe macropores. Table 1 summarizes the distributions that were used.

Admittedly, some of the assumptions are simplistic and may not reflect actual conditions in compacted soil liners. However, the simplifications were necessary to keep the analyses tractable and practical. The reader should consider the assumptions employed when interpreting results obtained with the models and their application to actual field conditions.

CONCLUSION

The models that have been described in the present paper were developed to evaluate how the variability of compacted soil affects the performance of compacted soil liners. The models are intended to bracket the possible patterns of flow that may occur in the field; one-dimensional flow in a continuum and three-dimensional flow in a network of macropores. In the companion paper (Benson and Daniel 1994), the models are used to evaluate the minimum thickness of soil liners that is necessary to ensure adequate hydraulic performance.

Based on previous studies, flow in compacted soil was assumed to exhibit different patterns that depend on the methods of processing and compacting the soil. For soil liners that are constructed with deformable clods and heavy construction machinery, the flow field was assumed to be a continuum because the scale at which the flow field is viewed is much larger than the size and spacing of the interclod pores. For liners constructed of large, stiff clods and lightweight machinery, the flow was assumed to occur primarily in macropores within the lifts that are interconnected and form continuous pathways. The models described in the present paper were developed to bracket these patterns of flow.

Previous studies have also shown that hydraulic conductivity of compacted soil is spatially variable, which renders deterministic analyses of soil liners difficult because the uncertainty of the soil properties is not incorporated rigorously. In the present paper, stochastic methods have been used to incorporate spatial variability and uncertainty in a rigorous manner.

It was found in this study that stochastic models can be developed that incorporate spatial variability and uncertainty in hydraulic conductivity and approximate the patterns of flow expected in soil liners. Two models have been presented in this paper. One model simulates one-dimensional flow in a spatially variable continuum. The other model approximates flow in a spatially variable network of interconnected macropores. In both models, distributions of first-passage time and flux were determined.

ACKNOWLEDGMENT

This research was funded by the U.S. Environmental Protection Agency (EPA) through Cooperative Agreement CR 0055586-01. This paper has not been subjected to EPA's peer review, and the opinions expressed herein do not necessarily reflect those of EPA.

APPENDIX I. REFERENCES

Aitchison, J., and Brown, J. (1957). *The lognormal distribution with special reference to its use in economics*. Cambridge University Press, Cambridge, England.

Albrecht, K. A., et al. (1989). "Excavation of an instrumented earthen liner: inspection of dyed flow paths and morphology." *Hazardous Waste and Hazardous Mat.*, 6(3), 269–279.

Anderson, D. C., et al. (1991). "Factors controlling the minimum soil liner thickness." *Draft Rep. No. EPA/600/2-91/008*. U.S. Environmental Protection Agency, Cincinnati, Ohio.

Ang, A., and Tang, W. (1975). "Basic principles." *Probability concepts in engineering planning and design*, Vol. 1, John Wiley and Sons, New York, N.Y.

Benson, C. H. (1989). "A stochastic analysis of water and chemical flow in compacted soil liners," PhD dissertation, Univ. of Texas at Austin, Austin, Tex.

Benson, C. H., and Daniel, D. E. (1990). "Influence of clods on hydraulic conductivity of compacted clay." *J. Geotech. Engrg.*, ASCE, 116(8), 1231–1248.

Benson, C. H., and Daniel, D. E. (1994). "Minimum thickness of compacted soil liners: II. results and case history." *J. Geotech. Engrg.*, ASCE, 120(1), 153–172.

Bogardi, I., Kelly, W., and Bardossy, A. (1989). "Reliability model for soil liner: initial design." *J. Geotech. Engrg.*, ASCE, 115(5), 658–669.

Catalán, J. M., and Cornell, C. A. (1976). "Earth slope reliability by a level-crossing method." *J. Geotech. Engrg. Div.*, ASCE, 102(6), 591–604.

Churchill, R. V. (1972). *Operational mathematics*. McGraw-Hill Book Co., New York, N.Y.

Corey, A. T. (1977). *Mechanics of fluids in heterogeneous porous media*. Water Resources Publications, Fort Collins, Colo.

Elsbury, B., and Sraders, G. (1989). "Building a better landfill liner." *Civil Engrg.*, ASCE, 59(4), 57–59.

Freeze, R. A. (1975). "A stochastic-conceptual analysis of one-dimensional groundwater flow in nonuniform homogeneous media." *Water Resour. Res.*, 11(5), 725–741.

Freeze, R. A., and Cherry, J. (1979). *Groundwater*. Prentice-Hall, Englewood Cliffs, N.J.

Goldman, L. J., et al. (1988). "Design, construction, and evaluation of clay liners for waste management facilities." *EPA/530/SW-86/007F*. U.S. Environmental Protection Agency, Washington, D.C.

Grimmett, G. R., and Stirzaker, D. R. (1982). *Probability and random processes*. Claredon Press, Oxford, England.

Hachich, W., and Vanmarcke, E. H. (1984). "Probabilistic updating of pore pressure fields." *J. Geotech. Engrg.*, ASCE, 109(3), 373–387.

Johnson, G. W., Crumbley, W., and Boutwell, G. (1990). "Field verification of clay liner hydraulic conductivity." *Waste containment systems: construction, regulation, and performance, GSP No. 26*. R. Bonaparte, ed., ASCE, New York, N.Y., 226–245.

Krapac, I. G., et al. (1989). "Hydraulic properties of an experimental soil liner: Preliminary results." *Proc., 12th Annu. Madison Waste Conf.*, Univ. of Wisconsin Extension, Madison, Wis., 395–411.

Press, W. H., Flannery, B., Teukolsky, S., and Vetterling, W. (1986). *Numerical recipes—the art of scientific computing*. Cambridge University Press, Cambridge, England.

Richards, P., and Thompson, C. (1989). "Permeability protocol for the compacted clay liner at the metropolitan Toronto Keele Valley landfill." *Can. J. Civ. Engrg.*, 16(4), 552–559.

Rogowski, A. S. (1990). "Relationship of laboratory- and field-determined hydraulic conductivity in compacted clay layer," *EPA/600/2-90;0225*. U.S. Environmental Protection Agency, Cincinnati, Ohio.

Ronold, K. O. (1990a). "Random field modeling of foundation failure modes." *J. Geotech. Engrg.*, ASCE, 116(4), 554–570.

Ronold, K. O. (1990b). "Reliability analysis of tension pile." *J. Geotech. Engrg.*, ASCE, 116(5), 760–773.

Streeter, V., and Wylie, E. (1979). *Fluid mechanics*. McGraw-Hill, Inc., New York, N.Y.
Vanmarcke, E. H. (1977a). "Probabilistic modeling of soil profiles." *J. Geotech. Engrg. Div.*, ASCE, 103(11), 1227–1246.
Vanmarcke, E. H. (1977b). "Reliability of earth slopes." *J. Geotech. Engrg. Div.*, ASCE, 103(11), 1247–1265.
Wu, T. H., and Kraft, L. M. (1967). "The probability of foundation safety." *J. Soil Mech. and Found. Div.*, ASCE, 93(5), 213–231.

APPENDIX II. NOTATION

The following symbols are used in this paper:

A = cross-sectional area of liner for analysis;
A_c = cross-sectional area of channels in partition;
C_{vx} = coefficient of variation of random process X;
$f_X(x)$ = probability density function for random process X;
h_{1j} = total head at top of jth channel;
h_{2j} = total head at bottom of jth channel;
H_{ik} = hydraulic head at point k in ith interlift zone;
H_L = depth of liquid covering liner;
I = average hydraulic gradient;
J_j = flow coefficient for channel j;
K = hydraulic conductivity;
K_{eq} = equivalent hydraulic conductivity;
L = thickness of lift;
N = number of lifts;
n_e = effective porosity;
N_c = number of channels in partition;
N_i = number of channels in ith interlift zone;
N_p = number of partitions;
Q_j = flow rate in jth channel;
R = hydraulic resistivity;
r_j = radius of jth channel;
r_{jk} = radial distance between point k and jth channel;
S = length of side of partition;
T = first-passage time;
T_d = deterministic first-passage time;
t_j = time of travel in jth channel;
t_{jk} = time of travel between channels j and k;
$T_r^{(i)}$ = transmissivity of ith interlift zone;
V_f = volumetric flux emanating from base of liner;
V_s = seepage velocity;
W_i = constant for Theim equation in ith interlift zone;
η_i = ith deterministic coefficient;
λ = mean number of channels/m^2;
σ_X^2 = variance of random process X;
τ = tortuosity; and
Φ_X = characteristic function for random process X.